

Theory for the Phonon Dispersion of Mixed-Valent $\text{Sm}_{0.75}\text{Y}_{0.25}\text{S}$

P. Entel, N. Grewe, M. Sietz, and K. Kowalski

Institut für Theoretische Physik der Universität zu Köln, D-5000 Köln 41, Germany

(Received 18 May 1979)

The phonon dispersion and elastic constants of mixed-valent $\text{Sm}_{0.75}\text{Y}_{0.25}\text{S}$ are calculated. The microscopic model takes into account interactions of localized $4f$ electrons with lattice vibrations and phonon-induced $4f \rightleftharpoons 5d$ transitions leading to a breathing of the rare-earth ionic radius. The resulting three-parameter model yields a quantitative overall agreement with quite anomalous experimental dispersion curves. As input data the unrenormalized frequencies are obtained from a second-neighbor Born-von Kármán model.

Among the many mixed-valent compounds (see recent reviews¹⁻⁴) $\text{Sm}_{1-x}\text{Y}_x\text{S}$ is known to possess interesting anomalies which are the subject of current research. Among these are special features of the T - x phase diagram^{5,6} (possibly two critical points), rather low values for the bulk moduli compared with SmS ,⁷ and the appearance of unusual soft LA phonons relative to the TA phonons.⁸ The latter effects are the subject of this paper in which we present a quantitative calculation of the phonon dispersions of $\text{Sm}_{0.75}\text{Y}_{0.25}\text{S}$. We use a microscopic model with four parameters, which is able to explain the underlying physics in a transparent way and has some advantages compared with other recent works.^{9,10} Since the unrenormalized phonon frequencies computed as input data presumably resemble very much those of the SmS constituent,¹¹ the strong renormalizations should mainly be due to the YS constituent which destroys the inversion symmetry of the NaCl lattice and thereby causes a drastic change of the $4f \rightleftharpoons 5d$ transition rate.^{12,13}

The following features of the measured dispersion curves of $\text{Sm}_{0.75}\text{Y}_{0.25}\text{S}$ (Ref. 8) are reproduced by our theory:

(i) LA phonons are unusually soft compared to

TA phonons. Nearly everywhere in the $[\xi\xi\xi]$ direction the LA branch lies below the TA branch, the difference being largest in the middle of the Brillouin zone. As one approaches point L , LA frequencies are extraordinarily enhanced until at point L itself we find normal behavior ($\nu_{\text{LA}} > \nu_{\text{TA}}$).

(ii) A similar behavior is seen along $[\xi\xi 0]$ where the LA branch lies below the TA_2 branch until they cross halfway between Γ and K .

(iii) The rather low LA sound velocities should lead to unusual magnitudes of the elastic constants (e.g., $C_{12} < 0$, indicating a tendency towards a structural instability of the system).

(iv) The LO phonons lie below the TO phonons. This effect is largest at point L .

These phonon phenomena are discussed within the framework of the periodic Anderson¹⁴ model extended to include the interaction of $4f$ electrons with longitudinal and transversal phonons (for early theories treating the mixed-valence phase in connection with the coupling of $4f$ electrons to a Bose field, we refer to Varma and Heine,¹⁵ Sherrington and Molnar,¹⁶ Haldane,¹⁷ and Entel, Leder, and Grewe¹⁸; for details of the present theory, see Grewe¹⁹).

With use of the following form for the electronic part of the Hamiltonian,

$$H_{\text{el}} = \sum_{\mathbf{k}, \sigma} \epsilon_{\mathbf{k}} d_{\mathbf{k}\sigma}^\dagger d_{\mathbf{k}\sigma} + \sum_{i, \sigma} E_{\sigma} f_{i\sigma}^\dagger f_{i\sigma} + \frac{1}{\sqrt{N}} \sum_{i, \mathbf{k}, \sigma} V [\exp(-i\mathbf{k} \cdot \mathbf{R}_i) f_{i\sigma}^\dagger d_{\mathbf{k}\sigma} + \text{H.c.}], \quad (1)$$

the unusual coupling of strongly localized $4f$ electrons to lattice vibrations can formally be derived by expanding the hybridization constant V (between $4f$ and $5d/6s$ states) and the position E_{σ} of the $4f$ level in the relative displacements of the neighboring ions:

$$V = V_0 + g_2 \sum_n \vec{\xi}_n \cdot \vec{e}_n + \sum_{n, n'} \vec{\xi}_n \hat{g}^{nn'} \vec{\xi}_{n'}, \quad E_{\sigma} = E_{0\sigma} + g_1 \sum_n \vec{\xi}_n \cdot \vec{e}_n + \dots \quad (2)$$

Since we are mainly interested in phonon phenomena, the Hubbard term is taken into account only in the Hartree-Fock approximation ($E_{0\sigma} = E_0 + U \langle n_{-\sigma}^f \rangle$). The displacements are split into a static and a fluctuating part due to phonons: $\vec{\xi}_n \cdot \vec{e}_n = -\Phi + \vec{\eta}_n \cdot \vec{e}_n$. Here Φ is the uniform part of the lattice distortion (relative change of the lattice constant) and may be regarded as the order parameter of the mixed-

valent phase. This scheme has successfully been used earlier in the description of continuous and discontinuous phase transitions in substituted SmS compounds.¹⁸⁻²⁰ The relative fluctuating displacements $\vec{\eta}_{i\sigma}$ of ions σ in cell l are given by phonon operators $b_{\vec{q},\lambda}$, $b_{\vec{q},\lambda}^\dagger$ in the usual way:

$$\vec{\eta}_{i\sigma} = \frac{1}{\sqrt{N}} \sum_{\vec{q},\lambda} \left(\frac{\hbar}{2M_\sigma 2\pi\nu_{\vec{q},\lambda}} \right)^{1/2} \epsilon_{\vec{q},\lambda}(\sigma) \exp(-i\vec{q} \cdot \vec{R}_{i\sigma}) (b_{\vec{q},\lambda} + b_{-\vec{q},\lambda}^\dagger), \quad (3)$$

where $\vec{\epsilon}_{\vec{q},\lambda}$ denotes the polarization vector and $\vec{R}_{i\sigma}$ the position vector of the σ th ion in the l th unit cell. The additional electron-phonon interaction arising from the presence of approximately 0.5 conduction electrons per lattice site is assumed to be absorbed in appropriate unrenormalized phonon frequencies. An evaluation of the self-energy contributions arising from the direct $4f$ -electron-phonon interaction (g_1 coupling term) and the strong coupling to $4f \rightleftharpoons 5d$ transitions (g_2 coupling term) then gives the renormalized frequencies. By taking only the lowest-order polarization diagram into account for the phonon self-energy $\Pi_{\vec{q},\lambda}(z)$, the new longitudinal modes (λ denotes LA or LO) are determined from $z^2 - \nu_{\vec{q},\lambda}^2 - 2\nu_{\vec{q},\lambda} \Pi_{\vec{q},\lambda}(z) = 0$. It has been shown that higher-order contributions do not qualitatively change the result for $\Pi_{\vec{q},\lambda}(z)$.²¹ An approximative solution of the integral equation is obtained by using piecewise-flat electronic bands. This is justified for \vec{q} not too small. Within this approach the final result for the longitudinal modes is²¹

$$[\nu^\lambda(\vec{q})]^2 = \frac{1}{2} \{ \nu_{\vec{q},\lambda}^2 + 4\tilde{V}^2 - [(\nu_{\vec{q},\lambda}^2 - 4\tilde{V}^2)^2 + 8\nu_{\vec{q},\lambda} \tilde{V} \tilde{g}_1^2 |T_{\vec{q},\lambda}|^2 F_{\vec{q}}(T)]^{1/2} \}. \quad (4)$$

The determination of the unrenormalized frequencies $\nu_{\vec{q},\lambda}$ is described below. \tilde{V} is the effective hybridization energy of $4f$ and $5d$ states, $V = \hbar \tilde{V} = V_0 - 2g_2 \Phi(T)$, where $\Phi(T) = [a(T) - a_0]/a_0$, the relative change of the lattice constant.²⁰ Since, in the undistorted lattice, parity conservation does not allow for a hybridization of $4f$ and $5d$ states at the same rare-earth ion, V_0 has from next-nearest neighbors a contribution of the form¹⁸: $\frac{1}{6} V_0 (\cos \frac{1}{2} k_x a \cos \frac{1}{2} k_y a + \cos \frac{1}{2} k_x a \cos \frac{1}{2} k_z a + \cos \frac{1}{2} k_y a \cos \frac{1}{2} k_z a)$. The form factor $T_{\vec{q},\lambda}$ is given by²¹

$$T_{\vec{q},\lambda} = \sum_{i',\sigma'} \left(\frac{\hbar}{2M_{\sigma'} M_{\text{RE}} 2\pi\nu_{\vec{q},\lambda}} \right)^{1/2} \left\{ M_{\text{RE}}^{1/2} \vec{\epsilon}_{\vec{q},\lambda}(\sigma') \exp[-i\vec{q}(\vec{R}_{i',\sigma'} - \vec{R}_{i0})] - M_{\sigma'}^{1/2} \epsilon_{\vec{q},\lambda}(0) \right\} \vec{e}_{i0}^{i'\sigma'}, \quad (5)$$

where $\vec{e}_{i0}^{i'\sigma'}$ is the unit vector from ion $(l, 0)$ to ion (l', σ') . The function $F_{\vec{q}}(T)$ contains phase-space factors and the expectation values $\langle f_{i\sigma}^\dagger f_{i\sigma} \rangle$ and $\alpha = \sum_{i\sigma} \langle f_{i\sigma}^\dagger d_{i\sigma} + \text{H.c.} \rangle$. Approximately they can be taken from a Hartree-Fock treatment of the extended periodic Anderson model describing the mixed-valent phase.¹⁸ The dependence of F on wave vector and temperature is weak and may be neglected. A typical value of $F_{\vec{q}}(T) = 0.1$ is used here.²² This leaves us with essentially two parameters, V and g_1 , which determine the magnitude of the renormalization of longitudinal lattice vibrations.

The transversal modes are affected by the part due to transversal displacements in the second-order term of the expansion (2) (see Grewe and Entel²³):

$$\nu^\lambda(\vec{q}) = \nu_{\vec{q},\lambda} (1 + 4|\alpha| S_{\vec{q},\lambda} / \nu_{\vec{q},\lambda})^{1/2}. \quad (6)$$

In view of the strong dependence of the hybridization mechanism on binding angles and local symmetries, the qualitative behavior of the coupling function is as follows:

(i) For TO phonons hybridization cannot be supported coherently by transversal motion which

makes the renormalization shift positive.

(ii) For TA phonons a coherent breathing of the $4f$ shell as a result of $4f \rightleftharpoons 5d$ transitions is energetically favorable and effectively decreases the TA-phonon frequencies. The unrenormalized phonon spectrum is calculated with a simple second-neighbor force-constant model appropriate to the semimetalliclike state of $\text{Sm}_{0.75}\text{Y}_{0.25}\text{S}$. Considering all possible central and noncentral nearest- and next-nearest-neighbor interactions in the regular fcc lattice with Sm and S ions constitutes a six-parameter model. The unrenormalized spectrum at 300 K is obtained with the following choice of force constants (in units of $4\pi^2$ dyn/cm is as follows: For central interactions, $V_{\text{SmS}} = 1100$, $V_{\text{SmSm}} = 150$, and $V_{\text{SS}} = 10$; for noncentral interactions, $V_{\text{SmS}'} = 50$, $V_{\text{SmSm}'} = 30$, and $V_{\text{SS}'} = 30$. These values for the force constants have been obtained by fitting the spectrum at those points in \vec{k} space where the renormalizations due to Eqs. (4) and (6) should be negligible. Because of the particular form of $T_{\vec{q},\lambda}$ LA phonons are not affected at the symmetry points X and L , whereas LO phonons are not affected at Γ and X but become

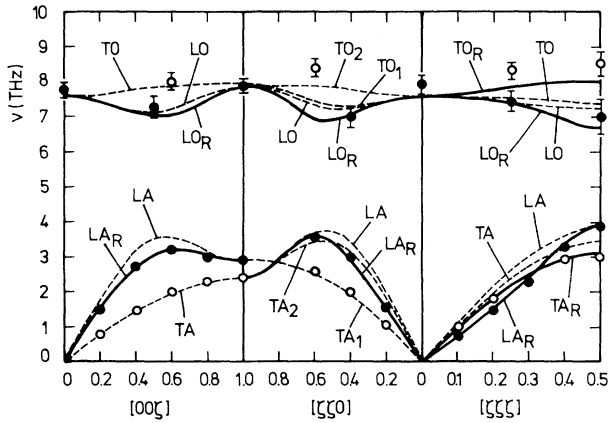


FIG. 1. Phonon dispersion curves for $\text{Sm}_{0.75}\text{Y}_{0.25}\text{S}$. The dashed curves represent the unrenormalized phonon spectrum obtained by a second-neighbor force-constant model. The full lines are the renormalized dispersion curves obtained with the help of Eqs. (2) and (5). The filled and open circles are experimental results for longitudinal and transversal branches, respectively.

unusually soft at L . The sound velocities in the different symmetry directions are strongly decreased. For TA phonons we expect no changes for small values of \bar{q} but for TA and TO phonons a large renormalization is predicted at L .^{11,21} This fixes the zeroth-order spectrum unequivocally. The dispersion curves thus obtained exhibit the normal behavior of phonons in semi-metals with fcc structure (dashed lines in Fig. 1). Remarkably, these phonon dispersions resemble what one expects for SmS, since the values for elastic constants and bulk modulus obtained from the force-constant model are in reasonable agreement with the values for SmS (Table I). This

gives a strong hint that, in addition to generating internal pressure, the Y constituent more drastically affects the properties of the compound. It is suggestive to assume an enhancement of the mixing strength V by on-site processes which are allowed in the absence of inversion symmetry due to the local distortions.

The renormalized phonon spectrum shown in Fig. 1 is in excellent agreement with experimental results: The observed anomalies of the dispersion curves, listed above, are well reproduced. Moreover, the same values $V_0 = 0.1373$ eV, $2g_2\Phi(T=300\text{ K}) = 0.0515$ eV, $g_1 = 0.065$ eV/Å, and $F_{\bar{q}}(T) = 0.1$ used here have already been chosen earlier in the description of realistic first-order phase boundaries of substituted SmS compounds.^{18,20} A shift of transversal branches has been taken into account only in the $[\zeta\zeta\zeta]$ direction. We have also calculated the temperature dependence of longitudinal-phonon frequencies in the $[\zeta\zeta\zeta]$ direction due to the temperature dependence of Φ : Over a wide range and not in the immediate vicinity of the phase transition, $\Phi(T)$ approximately depends linearly on T . This gives the numerical results shown in Fig. 2 [$2g_2\Phi(T=200) = 0.036$ eV, $V_{\text{SmS}} = 1400$]. The curves agree qualitatively with the experimental findings at low temperatures and are easily explained. With decreasing temperatures one approaches the first-order phase boundary which is accompanied by a decrease of V and hence—because of the particular form of Eq. (4)—by a decrease of ν^{LA} .

In conclusion, it has been shown that the theory of phonon renormalizations in mixed-valence compounds, as developed in Refs. 19 and 23, applied to a zeroth-order spectrum obtained by a

TABLE I. Elastic constants and bulk moduli for $\text{Sm}_{0.75}\text{Y}_{0.25}\text{S}$ (from the neutron-scattering data, Ref. 8) compared with those for $\text{Sm}_{0.7}\text{Y}_{0.3}\text{S}$ Ref. 7), for the zero-order spectrum obtained from the force-constant model, and for SmS and YS (Refs. 7 and 13). The lattice constant of $\text{Sm}_{0.75}\text{Y}_{0.25}\text{S}$ is taken to be (Ref. 7) $a = 5.73$ Å which gives the mean density $\rho = 5942$ g/cm³.

	C_{11}^a	C_{12}^a	C_{44}^a	B^a
$\text{Sm}_{0.75}\text{Y}_{0.25}\text{S}$	1.127	-0.413	0.29	0.1
$\text{Sm}_{0.7}\text{Y}_{0.3}\text{S}$	1.35 ± 0.1	-0.5 ± 0.1	0.3	0.1125
Zero-order spectrum	1.656	-0.141	0.278	0.458
SmS (mixed valent, $p = 6.5$ kbar)				0.52
SmS (semiconducting, $p = 0$)	1.2	0.11	0.25	0.47
YS	2.5	0.2	0.3	1.0

^a All quantities given in units of 10^{12} dyn/cm².

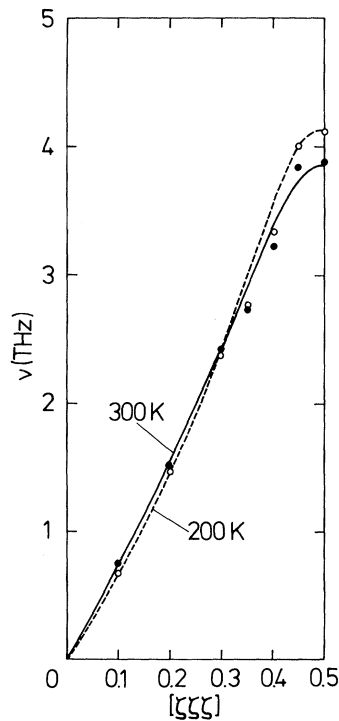


FIG. 2. Temperature dependence of the $[\xi\xi\xi]$ longitudinal-acoustical branch.

second-neighbor Born-von Kármán model qualitatively explains the experimental phonon dispersion of $\text{Sm}_{0.75}\text{Y}_{0.25}\text{S}$. The input spectra at the same time should show more similarity to the pure system SmS. In addition the data concerning the quite anomalous temperature dependence of LA-phonon frequencies could be reproduced. Arguments have been given as to why in this system the effects generally predicted for the mixed-valence situation should be particularly strong. However, it would be very useful to have more phonon data—dispersions, Debye-Waller factors, elastic constants, etc.—from other systems in order to test the concepts developed.

¹C. M. Varma, *Rev. Mod. Phys.* **48**, 219 (1976).

²*Valence Instabilities and Related Narrow Band Phenomena*, edited by R. D. Parks (Plenum, New York, 1977).

³J. H. Jefferson and K. W. H. Stevens, *J. Phys. C* **11**, 3919 (1978).

⁴J. M. Robinson, *Phys. Rep.* **51**, 1 (1979).

⁵T. Penney and F. Holtzberg, *Phys. Rev. Lett.* **34**, 322 (1975).

⁶A. Jayaraman, P. D. Dernier, and L. D. Longinotti, *Ref. 2*, p. 61.

⁷P. D. Dernier, W. Weber, and L. D. Longinotti, *Phys. Rev. B* **14**, 3635 (1976).

⁸H. A. Mook, R. M. Nicklow, T. Penney, F. Holtzberg, and M. W. Shafer, *Phys. Rev. B* **18**, 2925 (1978).

⁹K. H. Bennemann and M. Avignon, to be published.

¹⁰H. Bilz, private communication.

¹¹For a comparison of SmS- and Y-doped SmS and its relation to phononic peculiarities, see G. Güntherodt, R. Keller, P. Grünberg, A. Frey, W. Kress, R. Merlin, W. B. Holzappel, and F. Holtzberg, *Ref. 2*, p. 321.

¹²C. M. Varma, *Ref. 2*, p. 201.

¹³R. Keller, G. Güntherodt, W. B. Holzappel, M. Dietrich, and F. Holtzberg, *Solid State Commun.* **29**, 753 (1979).

¹⁴P. W. Anderson, *Phys. Rev.* **124**, 41 (1961).

¹⁵C. M. Varma and V. Heine, *Phys. Rev. B* **11**, 4763 (1975).

¹⁶D. Sherrington and S. Molnar, *Solid State Commun.* **16**, 1347 (1975).

¹⁷F. D. M. Haldane, *Phys. Rev. B* **15**, 281, 2477 (1977).

¹⁸P. Entel, H. J. Leder, and N. Grewe, *Z. Phys. B* **30**, 277 (1978).

¹⁹N. Grewe and P. Entel, *Z. Phys. B* **33**, 331 (1979).

²⁰P. Entel and N. Grewe, to be published.

²¹N. Grewe, P. Entel, and H. J. Leder, *Z. Phys. B* **30**, 393 (1978).

²²In the Hartree-Fock calculation the number of electrons per lattice site was fixed in such a way that the chemical potential lies in the lower band below the hybridization gap $2V$, thus simulating the semimetallic character of $\text{Sm}_{0.75}\text{Y}_{0.25}\text{S}$ in the mixed- and nonmixed-valent phase. The semimetallic character of both phases is consistent with resistivity measurements [T. Penney and F. Holtzberg, *Phys. Rev. Lett.* **34**, 322 (1975)].

²³N. Grewe and P. Entel, to be published.